The Thermo-Mechanical Stress Issues in a Thermally Enhanced QFP

Jack G. Hwang, T. J. Huang, and J. J. Lee

Advanced Semiconductor Engineering, Inc.
26, Chin 3rd Rd., Nantze Export Processing Zone
Kaohsiung, Taiwan, R.O.C.

1. Abstract

A finite element model with multiple load steps for different processes is used to predict the stresses in die in a thermally enhanced QFP (HQFP). In this model, non-stress-free initial condition and chemical shrinkage are implemented in this work to analyze thermo-mechanical stress issues occurring in HQFP. These issues emerge because of the presence of imperfect planarity of the upper surface of heat slug or the use of heat slug with various material. It was found that the x-component of normal stress at the center of die increases about 50% in the imperfect planarity case at the molding process, when compared to the perfect planarity case,. This significant increment of normal stress in x-direction leads to the increase of die-crack potential at the center if a pin mark is present. To reduce stresses, a more stringent control on the planarity of the heat slug and the use of a strengthened material are necessary. Another alliterative for reducing stresses is to use a stiffer material as heat slug. This can be accomplished by using copper instead of aluminum.

2. Introduction

To enhance the thermal performance of a modern package with high density of integrated circuit (IC), exposed heat slug or heat spreader has been implemented extensively for years in the package design. One of the examples is the thermally enhanced quad flat package (HQFP) which is widely adopted in the industry due to the low-cost consideration.

The thermal efficiency of HQFP with various designs of heat slug has been extensively studied [1,2,3]. For example, for a 28mmx28mm HQFP, Shaukatullah, *et al*. [1] measured a 22% reduction of thermal resistance in a natural convection condition at 1 W power when an exposed heat spreader was used. Ohtaka and his co-workers [2] proposed a low-cost leadframe with a heat spreader in the same size of HQFP (28mmx28mm) which can reduce the thermal resistance by 63% of that for a conventional QFP.

Although the studies showed that the addition of heat spreader/slug in a conventional package such as QFP can effectively enhance thermal performance, the thermo-mechanical stresses within the package due to the coefficient of thermal expansion (CTE) mismatch between respective materials become another critical issues [4,5,6]. In the study of Laurene and his co-worker [4], two types of molding compound was evaluated by comparing the warpages of conventional QFP and the electrically and thermally enhanced QFP (ETE-QFP) as they cooled from molding temperature to room temperature. The evaluation showed that the average warpages for ETE-QFP was about 65% higher than the conventional QFP. It also showed that the package warpage was reduced 60% for both conventional QFP and ETE-QFP when low stress compound was applied. These studies implied that the addition of heat slug or heat spreader will lead to the increase of stresses in such thermally or electrically enhanced package.

Finite elements models were used in the prediction of package warpage for years in the industry. In most of the models, the following assumptions are commonly adopted:

1. package is undeformed and is stress free during the molding process.
2. the mismatches of each material in the package is a function of material's CTE and temperature drop only.
3. materials are linear elastic and the corresponding mechanical properties are independent.

However, from the measurement data and predicted results, Kelly *et al*. [5,6] concluded that

at the presence of heat spreader/slug the first and the second assumptions are not valid because the package is significantly deformed due to the chemical shrinkage of the molding compound at the molding temperature. They explained that the chemical shrinkage plays a major role in the package warpage during the curing process, due to the asymmetry of the molding compound in a HQFP. Thus, in this study, the chemical shrinkage will be taken into consideration.

In our experiments, die cracks were observed in HQFP. Several factors are suspected to be responsible for such cracks, including the imperfect planarity of the upper surface of heat spreader, the weak structure of the heat slug, the large chemical shrinkage of molding compound, and the presence of pin marks on the die lower surface. In the study, these factors will be considered individually. Since two-dimensional plain strain models are used in these calculations, the x-component of normal stress (σ_{XX}) in die would be addressed to reflect the potential of crack (Mode I) occurrence.

4. Simulation Models

In this work, commercial code ANSYS 5.1 based on finite element models is used to carry out the stress predictions. The two-dimensional half model of 28x28x3.35mm QFPs without/with drop-in heat slug used in the computations are shown in Fig. 1. Model 1 represents a conventional QPT. To study the effect of the planarity, the models with perfect and imperfect planarity are presented in Model 2 and 3, respectively. A concavity on the upper surface of heat spreader caused by the manufacturing defect is used to simulate the imperfect planarity. This concavity has depth of $30\,\mu m$ and width $3.5\,mm$. A typical mesh for Model 2 used in the calculations is shown in Fig. 2. This mesh consists of about 19,000 nodes and 6,500 triangular or rectangular elements.

To consider the stresses at each manufacturing process, five load steps are considered,

1. Cool the leadframe with attached die from $T = 150^0 C$ to. $T = 25^0 C$
2. Preheat leadframe with attached die from $T = 25^0 C$ to $T = 175^0 C$, and put it on the drop-in heat spreader at $T = 175^0 C$.
3. Add molding compound into the package at $T = 175^0 C$.
4. Cool the package from $T = 175^0 C$ to $T = 25^0 C$.
5. Run IR reflow from $T = 25^0 C$ to $T = 225^0 C$.

At each load step, it is assumed that the mechanical properties of materials are linear elastic and independent of temperature; and the corresponding values are listed in Table 1 where E, ν and α represent the Young's modulus, Poisson's ratio and coefficient of thermal expansion, respectively.

Excepting Step 1, which is using the stress-free initial condition, each step uses the results from the previous step as initial conditions. At Step 3, the drop-in heat slug is initially undeformed, and the chemical shrinkage of molding compound is taken into account. As a result, for the 4th load step, a deformed package will be the initial condition.

Typically, the vendors of molding compound often quote the shrinkage value ranging from 0.24 to 0.50. This value consists of the shrinkages due to curing at $175^O C$ and temperature drop from $175^O C$ to room temperature. In this study, the degree of chemical shrinkage is simulated by the extra thermal shrinkage at the 3rd load step. For example, the amount of chemical shrinkage can be carried out by the temperature drop from $325^O C$ to $175^O C$. This makes the same amount as the thermal shrinkage due to the cooling process from molding temperature to room temperature.

4. Results & Discussions

Note that all the initial and boundary conditions were kept constant for all models at the 1st and 2nd load steps. This assumption results in same stress distributions for all the models at these two load steps.

4.1 The 1st and 2nd Load Steps

Fig. 3 and 4 represent the distribution of σ_{xx} in die for all the models at the 1st and 2nd load steps. As one can see from Fig. 3, the CTE mismatch between die, epoxy and leadframe (3.3, 135 and 17.6 $ppm/^0 C$, respectively) leads to a upward-bent die when the die-attached leadframe is cooled from bonding temperature to room temperature.

The CTE mismatch also results in high-tension stress on the upper surface, and compressive stress on the lower surface of die in x-direction. The exceeding tension stress on the upper surface might incur die crack. However, in reality, the downward die cracks are seldom observed. This could be attributed to the strengthened structure due to copper trace near the upper surface. The fracture mechanism of such strengthened structure has to be further verified from the fracture toughness tests. As the die-attached leadframe is preheated to molding temperature 175^0C and is placed on the drop-in heat slug, the CTE mismatch between materials creates an positive bending moment which leads to a upwardly deformed die, as shown in Fig. 4.

4.2 The 3rd Load Step

4.2.1 The effect of the imperfect planarity of the heat slug

As the chemical shrinkage of molding compound at molding temperature is taken into account, it results in compressive stress in x-direction on the upper surface of die and tension stress on the lower surface for both Model 2 and Model 3, as shown in Fig. 5. However, for Model 1, larger compressive stresses in x-direction on the upper surface are presented after the molding process. Also, the lower surface of die is acted by a compressive stress, too, which is different from those in Model 2 and 3. Obviously, the chemical shrinkage of the asymmetry of molding compound is responsible for this phenomenon. The distributions of x-component of normal stress on the lower surface of die for both models are further extracted from Fig. 5 and plotted in Fig. 6. It shows clearly that the imperfect planarity of the heat slug results in a significant increase of σ_{xx} (about 110%) near the central part of the die. From the distribution in Fig. 6, it can be realized that if there existing a concave surface near the center of heat slug, it can't offer a supporting force to the die when die is bending during the molding process. This implies that when the planarity of heat slug is not well controlled, exceeding stresses might exist in the package. If comparing σ_{xx} at the die center, it increases from about 25 Mpa to 38 Mpa (about 50% higher) after the molding process for imperfect heat slug case.

4.2.2 The effect of the material of the heat slug

It is suspicious that a softer material (with lower Young's modulus) such as aluminum is not appropriate to be used as heat slug. For this reason, a stiffer material, copper, is used as an alternative. To simulate the worst case, only Model 3 is considered. The resulted distributions of σ_{xx} on the lower surface of die is shown in Fig. 7.

It shows that if aluminum is used, σ_{xx} on the lower surface of the die will increase about 50% after the molding, whereas, slightly smaller σ_{xx}'s (about 2% less) are obtained when copper is used. This implies that the bending of the heat slug due to the chemical shrinkage of the compound is also responsible for the deformation of die. From this stress point of view, a stronger structure is always preferred to be the heat slug material.

4.2.3 The effect of the widths of concavity

Fig. 8 shows the distributions of σ_{xx} along the lower surface of die. In the figure, S presents the width of cave and is normalized to the die length. It shows that when $S \le 0.8$, the edge of the cave provides a supporting force to the die-pad. This force leads to the reduction of stress in die near the edge, which can be clearly seen in Fig. 8. For cases of $S \ge 0.8$, the edge of the cave starts to loss the support to the die-pad. Fox example, the unsupported die yields uniform stress distributions along the lower surface of the die in the case of $S = 0.9$ and $S = 1.1$. From the information above, one can concludes that the existence of the concave surface of the heat slug can results in a significant increment of stress, if the size of the concavity is about the size of die.

4.2.4 The effect of the pin mark

The theory of fracture mechanics indicates that longer length of the crack, larger stress intensity factor at the crack tip. Thus, if a deeper pin mark exist on the lower surface of the die, a larger K_I is expected. This implies that die tends to crack if there are pin makes on the lower surface of die.

In this study, an initial crack with length of 0.5% die highness at the die center is used to simulate the presence of the pin mark. The predicted K_I at the 2nd, the 3rd and the 5th load step for each model are shown in Table 3. This table gives the following information:

(1) If the planarity of the heat slug is perfect, K_I reduces at the end of the molding process when compared to that at the 2nd load step.

For example, K_I reduces to $0.95\,MPa\sqrt{m}$ after the molding process, when compared $0.14\,MPa\sqrt{m}$ before the molding process.

(2) If the planarity of the heat slug is imperfect, a 50% increase of K_I is obtained. For example, K_I is 0.14 and $0.21\,MPa\sqrt{m}$ before and after the molding process, respectively.

(3) If the fracture toughness K_C of the die is between 0.14 and $0.21\,MPa\sqrt{m}$, the crack of the die is likely propagating during the molding process.

4.2.5 The effect of the chemical shrinkage of the molding compound

In this work, the amount of the chemical shrinkage is simulated by the extra thermal shrinkage during the molding process. Thus, one can define the ratio of chemical shrinkage to thermal shrinkage,

$$K = \frac{\Delta T_{chemical}}{\Delta T_{thermal}} = \frac{\Delta T_{chemical}}{175^0 C - 25^0 C} = \frac{\Delta T_{chemical}}{150^0 C}$$

Fig. 9 shows the distributions of σ_{xx} along the lower surface of the die for cases with different K values. As one can see from this figure, higher chemical shrinkage of the molding compound yields a higher σ_{xx}. Thus, to relax the stresses in the die during the molding, a molding compound with smaller chemical shrinkage is preferred.

4.3 The 4th Load Step

When the package is cooled down from $T = 175^0 C$ to $T = 25^0 C$, the die is further contracted by the thermal shrinkage of molding compound. In addition, the faster contraction of leadframe and heat slug (compared to that of die) produces a bending moment to pull down the edges of die. Fig. 10 shows the resulted σ_{xx} for each model. It is noticed that the tension stresses on the lower surfaces of die in the HQFP cases change to compressive stresses due to the bending moment resulted from CTE mismatch in the package.

4.4 The 5th Load Step

The IR reflow process is the most severe condition for the package. The temperature increase from $25^0 C$ to $225^0 C$ leads to larger stresses in die than those in the molding process. The distributions of σ_{xx} in die for all the three models are shown in Fig. 11. It is found that, for the conventional QFP (Model 1), the expansion of molding compound acts more compressive stress on the die than any other model. Although the CTE mismatch between die and leadframe leads to a positive bending moment, the symmetrical expansion of molding compound restrains the amount of bending. Thus, no x-component tension stresses are observed on the lower surface of die in Model 1. However, for the HQFP models, the die is further compressed in the x-direction because of the expansion of compound on the upper surface. Take Model 3 for instance, the value of $(\sigma_{xx})_{\max}$ on the lower surface of die is 38 MPa at the molding process and is 65 MPa at the IR reflow process, corresponding to 70% increment. The existence of pin mark at die center might further endanger the die structure during IR-reflow process. For example, K_I is 50% more in Model 3 than in Model 2 (0.36 vs. $0.24\,MPa\sqrt{m}$) This indicates that the imperfect planarity of the heat slug might further endanger the die structure during the IR-reflow process.

5. Conclusions

1. The asymmetry of the molding compound in a HQFP results in the unbalanced contraction of expansion during the thermal loading. This leads to high stress in die.
2. When the planarity of the heat slug is not well controlled, adverse effect on the die stress will emerge, especially for those heat slugs with large concavity on the upper surface.
3. A stiffer material is more appropriate to be used as heat slug. Thus, the replacement of aluminum with copper as the heat slug material can effectively reduce stresses during the manufacturing processes.
4. The chemical shrinkage predominates the package deformation during the molding process. Thus, molding compound with low chemical shrinkage is suggested.
5. When a heat slug with concave upper surface is used, IR reflow process becomes a rigorous condition to the package, which may endanger

the package. The situation is even worse if there pin marks present on the lower surface of die.

6. References

1. H. Shaukatullah, M. A. Gaynes and L. H. White, "Thermal Enhancement of Surface Mount Electronic Packages with Heat Sinks", 43rd Electronic Components & Technology Conference, June 1-4, 1993, Orlando, Florida, pp. 256-263.
2. Ohtaka, Y. Kameyama, I. Yamagishi, T. Yonemoto and T. Suzumura, "High Performance, Low-Cost Leadframe with a Heat Spreader for HQFPs", Electronic Components & Technology Conference, pp. 682-686.
3. M. Karnezos, S. C. Chang, N. Chidambaram, C. M. Tak, A. S. Kyu and E. Combs, "EDQUAD-An Enhanced Performance Plastic Package", Electronic Components & Technology Conference, pp. 63-66.
4. L. Yip and A. Hamzehdoost, "Package Warpage Evaluation for High Performance PQFP", 45th Electronic Components & Technology Conference, pp. 229-233.
5. G. Kelly, C. Lyden, W. Lawton and J. Barrett, "Accurate Prediction of PQFP Warpage", 44th Electronic Components & Technology Conference, pp. 102-106.
6. G. Kelly, C. Lyden, W. Lawton and J. Barrett, "The Importance of Molding Compound Chemical Shrinkage in the Stress and Warpage Analysis of PQFPs", 45th Electronic Components & Technology Conference, pp. 977-981.

(a) Model 1

(b) Model 2

(c) Model 3

Fig. 1 Models of QFP-208 (28x28x3.35 mm)— (a) without heat slug; addition of heat slug (b) with perfect planarity, (c) with imperfect planarity.

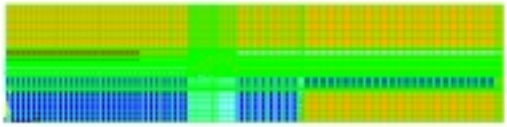

Fig. 2 mesh in the Model 2 for the calculation.

Fig. 3 The distribution of σ_{xx} in die at the 1st load step.

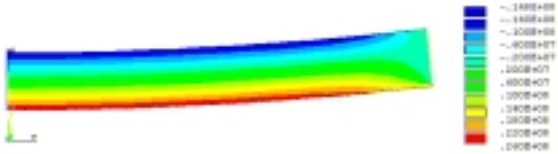

Fig. 4 The distribution of σ_{xx} in die at the 2nd load step.

(a)

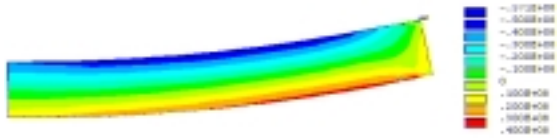

(b)

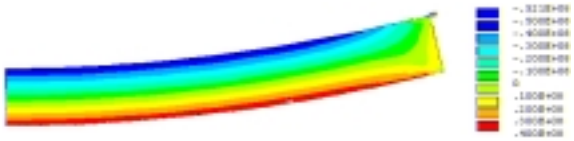

(c)

Fig. 5 The distributions of σ_{xx} in die at the 3rd load step for (a) Model 1; (b) Model 2; (c) Model 3.

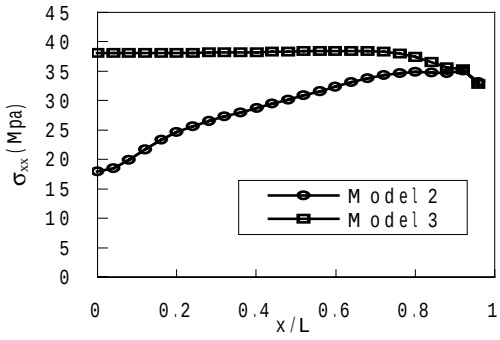

Fig. 6 σ_{xx} along the lower surface of die at the 3rd load step.

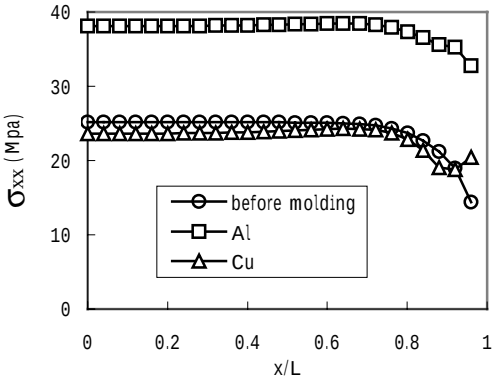

Fig.. 7 The comparison of σ_{xx} on the lower surface of die between the use of Al and Cu as the heat slug material at the end of molding process.

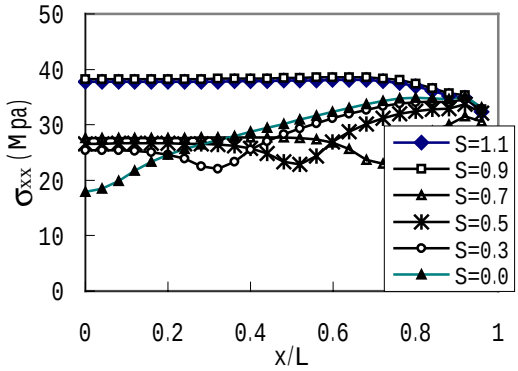

Fig. 8 σ_{xx} on the lower surface of die at the 3rd load step for various cave widths.

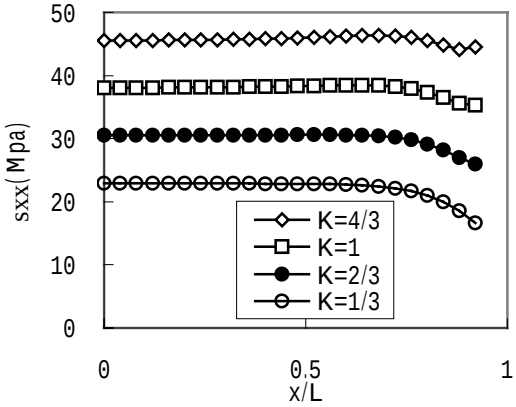

Fig. 9 The distributions of σ_{xx} along the lower surface of the die due to various degree of chemical shrinkage at the 3rd load step.

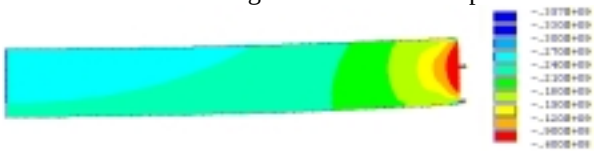

(a)

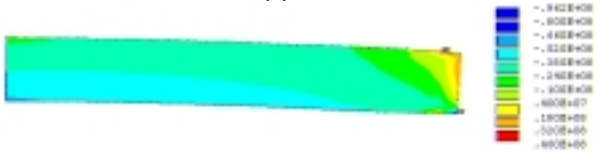

(b)

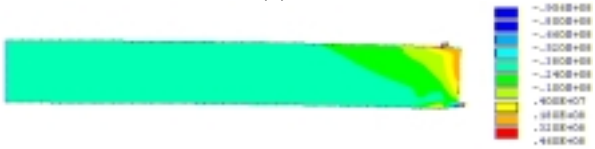

(c)

Fig. 10 The distributions of σ_{xx} in die at the 4th load step for (a) Model 1; (b) Model 2; (c) Model 3.

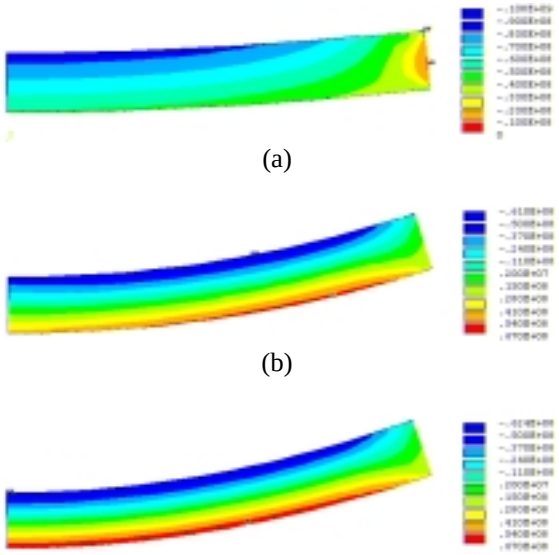

(a)

(b)

(c)

Fig. 11 The distributions of σ_{xx} in die at the 5th load step for (a) Model 1; (b) Model 2; (c) Model 3.

	$E(GPa)$	ν	$\alpha(ppm/^oC)$
Heat Slug, aluminum	70	0.33	23
Copper	132	0.30	17.6
Epoxy	7.0	0.35	135
Die	131	0.28	3.3
Molding Compound	20.6	0.27	16

Table 1 Data for each material used in the computations.

Model	K_I $(MPa\sqrt{m})$		
	2nd step	3rd step	5th step
2	0.14	.095	0.24
3	0.14	0.21	0.36

Table 2 The stress intensity factors for each model model in imperfect-contacted case.